

MECHANICAL ENGINEERING

Non-similar solutions of mixed convection flow from an exponentially stretching surface



P.M. Patil^{a,*}, D.N. Latha^a, S. Roy^b, Ebrahim Momoniat^c

^a Department of Mathematics, Karnatak University, Pavate Nagar, Dharwad 580 003, India

^b Department of Mathematics, I. I. T. Madras, Chennai 600 036, India

^c School of Computational and Applied Mathematics, University of Witwatersrand, Private Bag-3, Wits-2050, Johannesburg, South Africa

Received 25 May 2015; revised 7 September 2015; accepted 18 October 2015

Available online 23 December 2015

KEYWORDS

Double diffusive convection;
Non-similar solution;
Exponentially stretching sheet;
Chemical reaction;
Newton's linearization and finite difference scheme

Abstract In this paper we focus on to obtaining non-similar solutions for steady two dimensional double diffusive mixed convection boundary layer flows over an impermeable exponentially stretching sheet in an exponentially moving free stream under the influence of chemically reactive species. The nonlinear partial differential equations governing the flow, temperature and species concentration fields are presented in non-dimensional form with the help of suitable non-similar transformations. The resulting final non-dimensional set of coupled nonlinear partial differential equations is solved by using an implicit finite difference scheme in combination with the Newton's linearization technique. The effects of various non-dimensional physical parameters on velocity, temperature and species concentration fields are discussed. The results reveal that the streamwise coordinate ξ remarkably influences the flow, thermal and solutal concentration fields which display the existence of non-similar solutions.

© 2015 Ain Shams University. Production and hosting by Elsevier B.V. This is an open access article under the CC BY-NC-ND license (<http://creativecommons.org/licenses/by-nc-nd/4.0/>).

1. Introduction

Self-similar solutions for the coupled momentum, thermal and species concentration boundary layers over flat surfaces

are presented comprehensively in the convective heat and mass transfer text books by Incropera et al. [1] and Bejan [2]. Bejan [2] has suggested a similarity temperature variable which reduces the energy equation to an ordinary differential equation. Soundalgekar and Murty [3] have examined the effects of power law surface temperature variation on the heat transfer from a continuous moving surface with constant surface velocity. Similarity solutions were reported by Ali [4] for the case of a power-law surface velocity and three different thermal boundary conditions. Moutsoglou and Chen [5] have considered buoyancy effects on the flow and heat transfer from an inclined continuous sheet with either uniform wall temperature or uniform surface heat flux.

* Corresponding author.

E-mail addresses: pmpmath@gmail.com, pmpatil@kud.ac.in (P.M. Patil), sjroy@iitm.ac.in (S. Roy), Ebrahim.Momoniat@wits.ac.za (E. Momoniat).

Peer review under responsibility of Ain Shams University.



Production and hosting by Elsevier

Nomenclature

C	species concentration	T_w	temperature at the wall (K)
C_f	local skin-friction coefficient	T_∞	ambient temperature of the fluid (K)
C_p	specific heat at constant pressure	u	velocity component in the x direction (m s^{-1})
C_w	concentration at the wall	v	velocity component in the y direction (m s^{-1})
C_∞	ambient species concentration	x, y	Cartesian coordinates (m)
D	mass diffusivity		
f	dimensionless stream function	<i>Greek symbols</i>	
F	dimensionless velocity	α	thermal diffusivity ($\text{m}^2 \text{s}^{-1}$)
g	acceleration due to gravity	β, β^*	volumetric coefficients of the thermal and concentration expansions, respectively
G	dimensionless temperature	Δ	chemical reaction parameter
Gr, Gr^*	Grashof numbers due to temperature and species concentration, respectively	ε	velocity ratio parameter
H	dimensionless species concentration	ξ, η	transformed variables
L	characteristic length (m)	μ	dynamic viscosity ($\text{kg m}^{-1} \text{s}^{-1}$)
N	ratio of buoyancy forces	ν	kinematic viscosity ($\text{m}^2 \text{s}^{-1}$)
Nu	Nusselt number	ρ	density (kg m^{-3})
Pr	Prandtl number (ν/α)	ψ	stream function ($\text{m}^2 \text{s}^{-1}$)
Re_L	Reynolds number		
Ri	Richardson number	<i>Subscripts</i>	
$R(x)$	variable chemical reaction rate	e	free stream condition
Sc	Schmidt number (ν/D)	w	conditions at the wall
Sh	Sherwood number	ξ, η	denote the partial derivatives with respect to these variables, respectively
T	temperature (K)		

Magyari and Keller [6] have examined the heat and mass transfer characteristics on boundary layer flow due to an exponentially continuous stretching sheet. An effect of suction on the heat transfer phenomena over an exponentially stretching continuous surface was examined by Elbashbeshy [7]. Partha et al. [8] have investigated the effects of viscous dissipation on the mixed convection heat transfer from an exponentially stretching surface. Al-Odat et al. [9] have studied the effects of magnetic field on the thermal boundary layer flow over an exponentially stretching continuous surface. Sajid and Hayat [10] have studied the influence of thermal radiation on the boundary layer flow due to an exponentially stretching sheet. Bidin and Nazar [11] obtained the numerical solutions of the boundary layer flow over an exponentially stretching sheet with thermal radiation. Dulal Pal [12] discussed the mixed convection heat transfer in the boundary layers on an exponentially stretching sheet with magnetic field. The effect of radiation on the MHD boundary layer flow due to an exponentially stretching sheet was investigated by Ishak [13]. Mukhopadhyay and Gorla [14] have examined the effects of partial slip on boundary layer flow past a permeable exponentially stretching sheet in the presence of thermal radiation. In all these studies, self-similar or locally similar solutions have been presented. Rehman et al. [15] have studied the boundary layer stagnation point flow of third grade fluid over an exponentially stretching sheet. Stagnation flow of couple stress nanofluid over an exponentially stretching sheet through porous medium was examined by Rehman et al. [16]. Rahman and Nadeem [17] have analyzed the heat transfer characteristics over a vertical exponentially stretching cylinder. Rehman et al. [18] have discussed the nanoparticle effect over the boundary layer flow from an exponentially stretching cylinder. Hayat et al. [19–21] have examined the effects of three

dimensional flows for MHD, viscoelastic and Eyring-Powell fluids over an exponentially stretching sheet. Flow of Casson nanofluid with viscous dissipation and convective conditions were studied by Hussain et al. [22].

Further, the phenomenon of chemically reactive species has special significance in chemical and hydrometallurgical industries. The formation of smog represents a first order homogeneous chemical reaction. For instance, one can take into account the emission of NO_2 from automobiles and other smokestacks. Thus, NO_2 reacts chemically in the atmosphere with unburned hydrocarbons (aided by sunlight) and produces peroxyacetylnitrate, which forms a layer of photo-chemical smog. Chemical reactions can be treated as either homogeneous or heterogeneous processes. It depends on whether they occur at an interface or as a single-phase volume reaction [23]. Patil and Kulkarni [24] have examined the effects of chemical reaction on free convective flow of a polar fluid through a porous medium in the presence of internal heat generation. Patil and Pop [25] have studied the effects of surface transfer on unsteady mixed convection flow over a vertical cone with chemical reaction. Effects of chemical reaction on mixed convection flow of a polar fluid through a porous medium in the presence of internal heat generation were examined by Patil et al. [26]. Hayat et al. [27] have analyzed the effects of temperature and concentration stratification of mixed convection flow of an Oldroyd-B fluid with thermal radiation and chemical reaction. Shehzad et al. [28] have discussed the stagnation point flow of thixotropic fluid with mass transfer and chemical reaction. Hayat et al. [29] have examined the effects of Soret and Dufour on three-dimensional flow over an exponentially stretching surface through a porous medium in the presence of chemical reaction and heat source/sink. Hsiao [30,31] analyzed the heat and mass transfer characteristics on mixed

convection for MHD viscoelastic fluid past a stretching sheet with Ohmic dissipation. Nanofluid flow with multimedia physical features for conjugate mixed convection and radiation was discussed by Hsiao [32]. Also, Hsiao [33] studied the MHD effects on mixed convection for viscoelastic fluid past a porous wedge.

The main objective of the present numerical investigation is to obtain non-similar solutions of double diffusive mixed convection boundary layer flow along a vertical semi-infinite impermeable exponentially stretching surface in an exponentially moving free stream under the influence of chemically reactive species.

2. Formulation of the problem

We consider a steady two-dimensional mixed convection boundary layer flow along a semi-infinite vertical impermeable exponentially stretching surface with velocity $U_w(x)$ moving in an exponentially free stream with velocity $U_e(x)$ in the positive x -direction of an incompressible viscous fluid of temperature T_∞ and concentration C_∞ , under the influence of chemically reactive species. The x -axis is taken along the plate in the vertically upward direction and the y -axis is taken normal to it. A schematic representation of the physical model and coordinates system is depicted in Fig. 1. The driving buoyancy force arises due to the temperature and concentration differences in the fluid. The concentration of diffusing species is assumed to be very small in comparison with other chemical species far away from the surface C_∞ . The physical properties of the fluid flow model are assumed to be constant except the density variations causing a body force in the momentum equation. The Boussinesq approximation is employed for the fluid properties to relate density changes, and to couple in this way the temperature and species concentration fields to the flow field [34]. Under these assumptions, the equations of conservation of

mass, momentum, energy and species concentration governing the mixed convection boundary layer flow over a vertical impermeable exponentially stretching surface are given by

$$\frac{\partial u}{\partial x} + \frac{\partial v}{\partial y} = 0, \tag{1}$$

$$u \frac{\partial u}{\partial x} + v \frac{\partial u}{\partial y} = U_e \frac{dU_e}{dx} + \nu \frac{\partial^2 u}{\partial y^2} + g[\beta(T - T_\infty) + \beta^*(C - C_\infty)], \tag{2}$$

$$u \frac{\partial T}{\partial x} + v \frac{\partial T}{\partial y} = \frac{\nu}{Pr} \frac{\partial^2 T}{\partial y^2}, \tag{3}$$

$$u \frac{\partial C}{\partial x} + v \frac{\partial C}{\partial y} = \frac{\nu}{Sc} \frac{\partial^2 C}{\partial y^2} - R(x)(C - C_\infty), \tag{4}$$

where all the parameters are defined in the nomenclature.

The physical boundary conditions are given by

$$\begin{aligned} y = 0 : u = U_w(x), \quad v = 0, \\ T = T_w = T_\infty + (T_{w0} - T_\infty) \exp\left(\frac{2x}{L}\right), \\ C = C_w = C_\infty + (C_{w0} - C_\infty) \exp\left(\frac{2x}{L}\right), \\ y \rightarrow \infty : u \rightarrow U_e(x), \quad T \rightarrow T_\infty, \quad C \rightarrow C_\infty. \end{aligned} \tag{5}$$

The stretching sheet velocity $U_w(x)$, free stream velocity $U_e(x)$ and variable chemical reaction rate $R(x)$ are respectively given by the following:

$$\begin{aligned} U_w(x) = U_0 \exp\left(\frac{x}{L}\right), \quad U_e(x) = U_\infty \exp\left(\frac{x}{L}\right) \\ \text{and } R(x) = R_0 \exp\left(\frac{x}{L}\right), \end{aligned}$$

where U_0 is the reference velocity, R_0 is constant, U_∞ is the free stream velocity and L is the characteristic length.

Using the following transformations

$$\begin{aligned} \xi = \frac{x}{L}, \quad \eta = \left(\frac{U_0}{\nu x}\right)^{1/2} \exp\left(\frac{x}{2L}\right)y, \\ \psi(x, y) = (\nu U_\infty x)^{1/2} \exp\left(\frac{x}{2L}\right)f(\xi, \eta), \\ T - T_\infty = (T_w - T_\infty)G(\xi, \eta), \\ (T_w - T_\infty) = (T_{w0} - T_\infty) \exp\left(\frac{2x}{L}\right), \\ C - C_\infty = (C_w - C_\infty)H(\xi, \eta), \\ (C_w - C_\infty) = (C_{w0} - C_\infty) \exp\left(\frac{2x}{L}\right), \\ u = \frac{\partial \psi}{\partial y}, \quad v = -\frac{\partial \psi}{\partial x}, \quad f_\eta(\xi, \eta) = F, \quad u = U_0 \exp\left(\frac{x}{L}\right)F, \\ v = -\left(\frac{\nu U_0}{x}\right)^{1/2} \exp\left(\frac{x}{2L}\right) \left\{ (1 + \xi) \frac{f}{2} + \xi f_\xi + \frac{x}{2} \eta \left(\frac{1}{L} - \frac{1}{x} \right) \frac{\partial f}{\partial \eta} \right\}, \end{aligned} \tag{6}$$

to Eqs. (1)–(4), we find that Eq. (1) is identically satisfied, and Eqs. (2)–(4) reduce

$$F_{\eta\eta} + (1 + \xi) \frac{f}{2} F_\eta - \xi F^2 + \xi Ri(G + NH) + \xi e^2 = \xi [FF_\xi - f_\xi F_\eta], \tag{7}$$

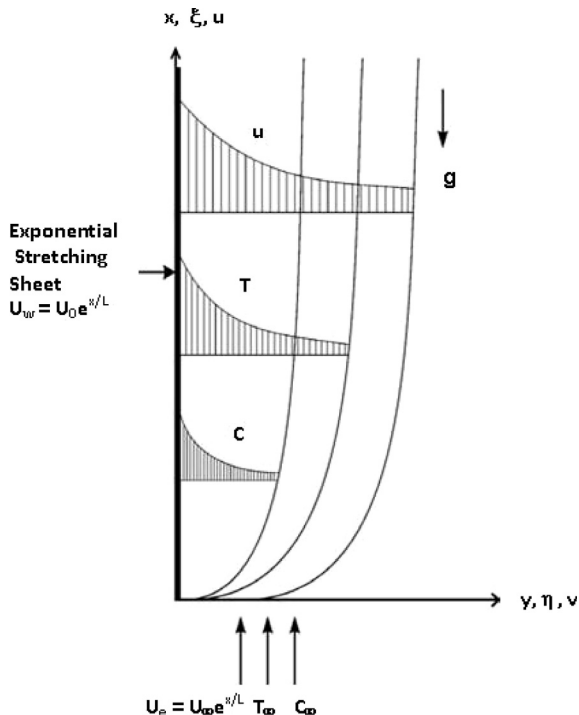


Figure 1 Schematic flow model and coordinate system.

$$G_{\eta\eta} + (1 + \xi) \frac{Pr_f}{2} G_\eta - 2Pr\xi FG = \xi Pr [FG_\xi - f_\xi G_\eta], \tag{8}$$

$$H_{\eta\eta} + (1 + \xi) \frac{Sc_f}{2} H_\eta - Sc\xi(2F + Re_L \Delta)H = \xi Sc [FH_\xi - f_\xi H_\eta]. \tag{9}$$

The physical boundary conditions (5) become

$$\begin{aligned} F(\xi, 0) = 1, \quad G(\xi, 0) = 1, \quad H(\xi, 0) = 1, \\ F(\xi, \eta) \rightarrow \varepsilon, \quad G(\xi, \eta) \rightarrow 0, \quad H(\xi, \eta) \rightarrow 0 \quad \text{as } \eta \rightarrow \infty. \end{aligned} \tag{10}$$

Here $f(\xi, \eta) = \int_0^\eta F d\eta + f_w$; where $f_w = 0$. The Richardson number, Ri , characterizes the relative importance of natural and forced convections and thus it is known as the mixed convection parameter, N is the dimensionless parameter representing the ratio between the thermal and the concentration buoyancy forces, and ε is the velocity ratio parameter which are defined as

$$Ri = \frac{Gr}{Re_L^2}, \quad N = \frac{Gr^*}{Gr} \quad \text{and} \quad \varepsilon = \frac{U_\infty}{U_0}, \tag{11}$$

where $Gr = g\beta(T_{w0} - T_\infty)L^3/v^2$ is the Grashof number referring to the wall temperature, $Gr^* = g\beta^*(C_{w0} - C_\infty)L^3/v^2$ is the Grashof number referring to the wall concentration and $Re_L = U_\infty L/v$ is the Reynolds number. It is worth mentioning here that $Ri > 0$ ($T_w > T_\infty$) corresponds to the heated surface, $Ri < 0$ ($T_w < T_\infty$) corresponds to the cooled surface and $Ri = 0$ ($T_w = T_\infty$) corresponds to the forced convection flow. The positive values of N ($N > 0$) imply that both buoyancy forces act in the same direction while the negative values of N ($N < 0$) appear when thermal and concentration buoyancy forces act in opposite directions. Also, $N \rightarrow 0$ for negligible buoyancy effect due to mass diffusion, and $N \rightarrow \infty$ for negligible buoyancy effect due to thermal diffusion. The chemically reactive species parameter Δ is representing the generation or consumption of the diffusing species. If Δ is positive (> 0) for species generation, it is negative (< 0) for species consumption and is zero for no chemical reaction.

The practical interest of physical quantities are the skin friction coefficient C_f , the Nusselt number Nu and the Sherwood number Sh , which represent the wall shear stress, the heat transfer rate and the mass transfer rate at the surface, respectively. These coefficients are defined as

$$C_f = \mu \frac{2(\partial u / \partial y)_{y=0}}{\rho U_w^2} = 2Re_L^{-1/2} \xi^{-1/2} F_\eta(\xi, 0) \tag{12}$$

$$\text{i.e., } (Re_L \xi \exp(\xi))^{1/2} C_f = 2F_\eta(\xi, 0),$$

$$Nu = -x \frac{(\partial T / \partial y)_{y=0}}{(T_w - T_\infty)} = -(Re_L \xi \exp(\xi))^{1/2} G_\eta(\xi, 0) \tag{13}$$

$$\text{i.e., } (Re_L \xi \exp(\xi))^{-1/2} Nu = -G_\eta(\xi, 0),$$

$$Sh = -x \frac{(\partial C / \partial y)_{y=0}}{(C_w - C_\infty)} = -(Re_L \xi \exp(\xi))^{1/2} H_\eta(\xi, 0) \tag{14}$$

$$\text{i.e., } (Re_L \xi \exp(\xi))^{-1/2} Sh = -H_\eta(\xi, 0).$$

3. Method of non-similar solution

The set of dimensionless nonlinear coupled partial differential Eqs. (7)–(9) under the boundary conditions (10) has been solved numerically by using an implicit finite difference scheme in combination with the Newton’s linearization technique. The advantage of this technique is that it has quadratic rate of convergence. Applying the Newton’s linearization technique [35–38] the nonlinear coupled system of partial differential equations is replaced by the following sequence of linear partial differential equations:

$$F_{\eta\eta}^{i+1} + X_1^i F_\eta^{i+1} + X_2^i F^{i+1} + X_3^{i+1} F_\xi^{i+1} + X_4^i G^{i+1} + X_5^i H^{i+1} = X_6^i, \tag{15}$$

$$G_{\eta\eta}^{i+1} + Y_1^i G_\eta^{i+1} + Y_2^i G^{i+1} + Y_3^i G_\xi^{i+1} + Y_4^i F^{i+1} = Y_5^i, \tag{16}$$

$$H_{\eta\eta}^{i+1} + Z_1^i H_\eta^{i+1} + Z_2^i H^{i+1} + Z_3^i H_\xi^{i+1} + Z_4^i F^{i+1} = Z_5^i. \tag{17}$$

The coefficient functions with iterative index i are known and the functions with iterative index $(i + 1)$ are to be determined. The boundary conditions are given by

$$\begin{aligned} F^{i+1}(\xi, 0) = 1, \quad G_\eta^{i+1}(\xi, 0) = 1, \quad H^{i+1}(\xi, 0) = 1, \\ F^{i+1}(\xi, \eta) = \varepsilon, \quad G^{i+1}(\xi, \eta) = 0, \quad H^{i+1}(\xi, \eta) = 0 \quad \text{at } \eta = \eta_\infty. \end{aligned} \tag{18}$$

The coefficients in Eqs. (15)–(17) are given by

$$X_1^i = (1 + \xi) \frac{f}{2} + \xi f_\xi; \quad X_2^i = -\xi(2F + F_\xi); \quad X_3^i = -\xi F;$$

$$X_4^i = \xi Ri; \quad X_5^i = \xi Ri N; \quad X_6^i = -\xi[(F + F_\xi) + \varepsilon^2];$$

$$Y_1^i = Pr \left[(1 + \xi) \frac{f}{2} + \xi f_\xi \right]; \quad Y_2^i = -2Pr\xi F; \quad Y_3^i = -Pr\xi F;$$

$$Y_4^i = -Pr\xi(2G + G_\xi); \quad Y_5^i = Y_4^i F;$$

$$Z_1^i = Sc \left[(1 + \xi) \frac{f}{2} + \xi f_\xi \right]; \quad Z_2^i = -Sc\xi(2F + Re_L \Delta);$$

$$Z_3^i = -Sc\xi F; \quad Z_4^i = -Sc\xi(2H + H_\xi); \quad Z_5^i = Z_4^i F.$$

The resulting sequence of linear partial differential Eqs. (15)–(17) was discretized using second order central difference formula in η -direction (boundary layer) and backward difference formula in ξ -direction (streamwise). In each iteration step, the equations were then reduced to a system of linear algebraic equations, with a block tri-diagonal structure which is solved using Varga’s algorithm [39]. To ensure the convergence of the numerical solution to the exact solution, step sizes $\Delta\eta$ and $\Delta\xi$ are optimized and the results presented here are independent of the step sizes at least up to the fifth decimal place. A convergence criterion based on the relative difference between the current and previous iteration values is employed. The solution is assumed to have converged and the iteration process is terminated when the difference reaches less than 10^{-5} , i.e.,

$$\begin{aligned} \text{Max}\{|(F_\eta)_w^{i+1} - (F_\eta)_w^i|, |(G_\eta)_w^{i+1} - (G_\eta)_w^i|, \\ |(H_\eta)_w^{i+1} - (H_\eta)_w^i|\} < 10^{-5}. \end{aligned} \tag{19}$$

4. Results and discussion

The numerical computations have been carried out for various values of the governing parameters involved in the physical problem, namely, $Ri(-2 \leq Ri \leq 5)$, $Sc(0.22 \leq Sc \leq 2.57)$, $\varepsilon(0.5 \leq \varepsilon \leq 1.5)$, $\Delta(-2 \leq \Delta \leq 2)$, $N(-2.0 \leq N \leq 2.0)$ and $\xi(0 \leq \xi \leq 1)$. The edge of the boundary layer (η_∞) has been taken between 4.0 and 10.0 depending on the values of the parameters. It may be noted that the range of parameter values is used for air and water at different temperatures. For example, $Pr = 0.7$ for air, $Pr = 7.0$ for water at 20 °C and the value of Pr reduces for water at higher temperature. In order to verify the accuracy of the presented approach, we have validated and compared some of steady state results of heat transfer rate $[-G_\eta(0)]$ by direct comparison with the results previously reported by Soundalgekar and Murty [3], Ali [4] and Moutsoglou and Chen [5]. Some of the comparisons are shown in Table 1 and are found to be in excellent agreement. In support of non-similar solutions the effects of Ri , N and ε , some of the other numerical results pertaining to skin-friction parameter $(Re_L \xi e^\xi)^{1/2} C_f$, heat transfer parameter $(Re_L \xi e^\xi)^{-1/2} Nu$ and mass transfer parameter $(Re_L \xi e^\xi)^{-1/2} Sh$ are tabulated in Table 2.

The effects of velocity ratio parameter (ε) and buoyancy (mixed convection or Richardson number) parameter (Ri) on velocity profiles $F(\xi, \eta)$ when $N = 0.5$, $Pr = 0.7$, $Sc = 2.57$, $\Delta = 1$, $Re_L = 1$ and $\xi = 0.5$ are displayed in Fig. 2. The influence of buoyancy assisting force ($Ri > 0$) displays the overshoot in the velocity profile $F(\xi, \eta)$ near the surface for both values of the velocity ratio parameter (ε) $\varepsilon = 1$ and $\varepsilon = 1.5$. The magnitude of velocity overshoots increases with the increase in buoyancy parameter ($Ri > 0$). The physical reason is that the assisting buoyancy force (Ri) acts like a supporting pressure gradient and enhances the magnitude of velocity pro-

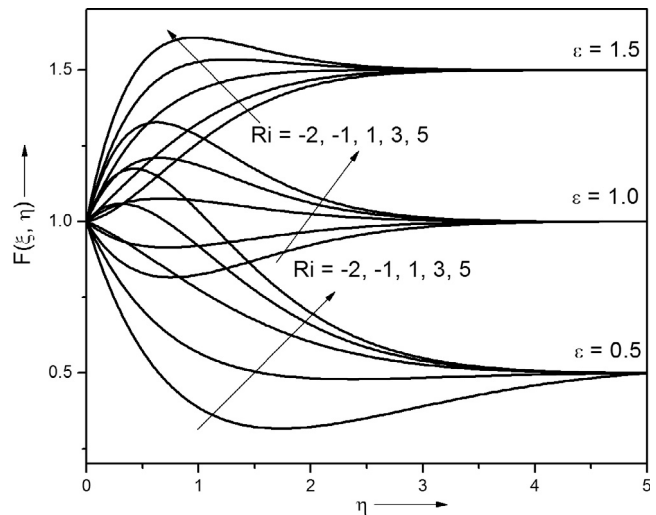


Figure 2 Effects of Ri and ε on velocity profile $F(\xi, \eta)$ for $N = 0.5$, $Pr = 0.7$, $Sc = 2.57$, $\Delta = 1$, $Re_L = 1$ and $\xi = 0.5$.

file $|F(\xi, \eta)|$ within the boundary layer. This causes a velocity overshoot within the boundary layer. The higher velocity overshoot is observed in the vicinity of the wall within the boundary layer for the case of $\varepsilon = 1.5$. It is interesting to note from Fig. 2 that the buoyancy opposing force ($Ri < 0$) reduces the magnitude of the velocity significantly within the boundary layer for all the values of velocity ratio parameter $\varepsilon = 0.5$, $\varepsilon = 1$ and $\varepsilon = 1.5$. The representative negative values of $Ri(Ri = -2, -1)$ are presented in Fig. 2 to limit the number of lines in this graph. However, for $\varepsilon < 1$, the back flow is observed near the surface considerably as it can be seen in Fig. 2. This may be due to the fact that the wall velocity U_w is dominating over the free stream velocity U_e . When $\varepsilon > 1$,

Table 1 Comparison of the steady state results $[-G_\eta(0)]$ for $Ri = 0$, $N = 0$, $\xi = 0$, $\varepsilon = 0$, $\Delta = 0$, $m = 0$ selected values of Pr to previously published work.

Pr	0.7	1.0	2.0	7.0	10	100
Soundalgekar and Murty [3]	0.3508	–	0.6831	–	1.6808	–
Ali [4]	0.3476	0.4416	–	–	1.6713	–
Moutsoglou and Chen [5]	0.34924	–	–	1.38703	–	–
Present work	0.354218	0.444430	0.683031	1.386868	1.680158	5.547516

Table 2 Steady state results of skin-friction parameter $(Re_L \xi e^\xi)^{1/2} C_f$, heat transfer parameter $(Re_L \xi e^\xi)^{-1/2} Nu$ and mass transfer parameter $(Re_L \xi e^\xi)^{-1/2} Sh$ for $\xi = 1.0$, $\Delta = 1.0$, $Sc = 2.57$, $Re_L = 1.0$ and $Pr = 0.7$.

Ri	N	ε	$(Re_L \xi e^\xi)^{1/2} C_f$	$(Re_L \xi e^\xi)^{-1/2} Nu$	$(Re_L \xi e^\xi)^{-1/2} Sh$
1.0	0.5	0.5	-0.252	1.203	2.862
1.0	0.5	1.0	0.896	1.304	2.944
1.0	0.5	1.5	2.544	1.410	3.045
3.0	0.5	0.5	1.544	1.291	2.959
3.0	0.5	1.0	2.570	1.370	3.024
3.0	0.5	1.5	4.096	1.460	3.111
1.0	1.5	0.5	0.186	1.220	2.883
1.0	1.5	1.0	1.313	1.317	2.962
1.0	1.5	1.5	2.936	1.420	3.060

the back flow is not much observed because the reason is that free stream velocity U_e slowly dominates over the wall velocity U_w . The driving buoyancy parameter (Ri) is relatively less influenced on the temperature and species concentration profiles ($G(\xi, \eta), H(\xi, \eta)$) and graphs are not presented here due to limit the number of graphs.

Figs. 3 and 4 present the effects of ratio of buoyancy forces parameter (N) and ratio of velocity parameter (ε) on the velocity profile $F(\xi, \eta)$ and skin friction parameter $((Re_L \xi e^\xi)^{1/2} C_f)$ for $Pr = 0.7$, $Sc = 2.57$, $\Delta = 1$, $Re_L = 1$. It is observed that the velocity profile increases as ratio of buoyancy forces parameter (N) increases for both values of velocity ratio parameter (ε) at $\varepsilon = 1$ and $\varepsilon = 1.5$. Further, skin friction parameter $((Re_L \xi e^\xi)^{1/2} C_f)$ increases with the increase in the ratio of buoyancy parameter (N). The physical reason is that the assisting ratio of buoyancy forces ($N > 0$) implies supporting pressure gradient and thus fluid gets up accelerated. This results into thinner momentum boundary layer and the skin

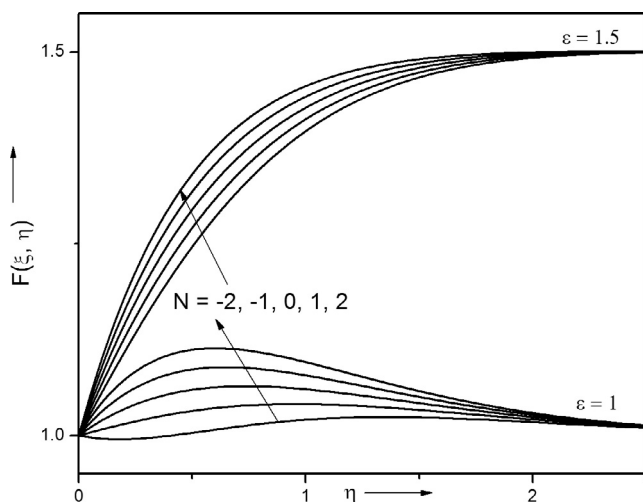


Figure 3 Effects of N and ε on velocity profile $F(\xi, \eta)$ for $Ri = 1$, $Pr = 0.7$, $Sc = 2.57$, $\Delta = 1$, $Re_L = 1$ and $\xi = 0.5$.

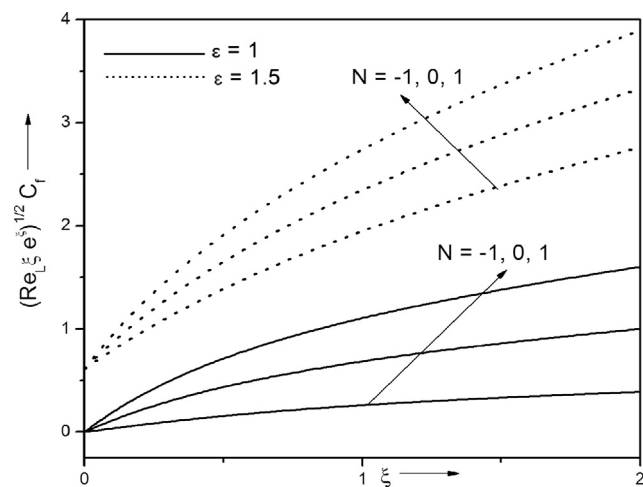


Figure 4 Effects of N and ε on skin friction $(Re_L \xi e^\xi)^{1/2} C_f$ for $Ri = 1$, $Pr = 0.7$, $Sc = 2.57$, $\Delta = 1$, and $Re_L = 1$.

friction parameter $((Re_L \xi e^\xi)^{1/2} C_f)$ increases. The results presented in Fig. 4 display that $((Re_L \xi e^\xi)^{1/2} C_f)$ increases with the increase in the velocity ratio parameter. To be more specific, in particular, when $\Delta = 1$, $Ri = 1$, $Re_L = 1$, $Sc = 2.57$, $Pr = 0.7$ at $\xi = 1.0$, $((Re_L \xi e^\xi)^{1/2} C_f)$ increases approximately about 199% and 240% as ε increases from 1.0 to 1.5 for $N = -1.0$ and 1.0, respectively (see Fig. 4).

The effects of Prandtl number (Pr) and the ratio of velocity parameter (ε) on the temperature profile ($G(\xi, \eta)$) at $\xi = 0.5$ are displayed in Fig. 5 for $\Delta = 1$, $Ri = 1$, $Re_L = 1$, $Sc = 2.57$, $Pr = 0.7$ and $N = 0.5$. The results presented in Fig. 5 indicate that the magnitude of the temperature profile decreases as Pr increases from $Pr = 0.7$ to $Pr = 7.0$ irrespective of the values of the ratio of velocity parameter. In the present case, higher Prandtl number (Pr) fluid (water, $Pr = 7.0$) is more viscous fluid which reduces the magnitude of velocity within the boundary layer as compared to lower (Pr) fluid (air, $Pr = 0.7$). It is also noticed in Fig. 5 that the magnitude of temperature profiles reduces more near the wall due to the increase in Prandtl number (Pr) from $Pr = 0.7$ to $Pr = 7.0$. This may be due to the fact that the effect of viscosity is more pronounced near the wall. Further, the temperature profile ($G(\xi, \eta)$) also reveals the fact that the effect of higher Prandtl number fluids (water, $Pr = 7.0$) results into a thinner thermal and species concentration boundary layers as compared to lower Pr fluid (air, $Pr = 0.7$). The physical reason is that the Prandtl number controls the relative thicknesses of the momentum and thermal boundary layers. For lower Pr fluids (air, $Pr = 0.7$) the heat diffuses very quickly compared to the momentum. Thus, for lower Pr fluids, the thickness of the thermal boundary layer is much bigger than the thickness of velocity boundary layer. Similarly, for higher Pr fluids (water, $Pr = 7.0$), the thickness of thermal boundary layer is much smaller than that of velocity boundary layer.

Fig. 6 illustrates the role of streamwise coordinate ξ on the velocity and temperature profiles ($F(\xi, \eta), G(\xi, \eta)$) when $Ri = 1.0$, $Re_L = 1$, $\Delta = 1$, $N = 0.5$, $Sc = 2.57$, $\varepsilon = 1.5$ and $Pr = 0.7$. The velocity profile increases near the plate remarkably within the momentum boundary layer when streamwise coordinate ξ increases from $\xi = 0$ to $\xi = 1$ whereas temperature profile ($G(\xi, \eta)$) decreases with the increase in streamwise

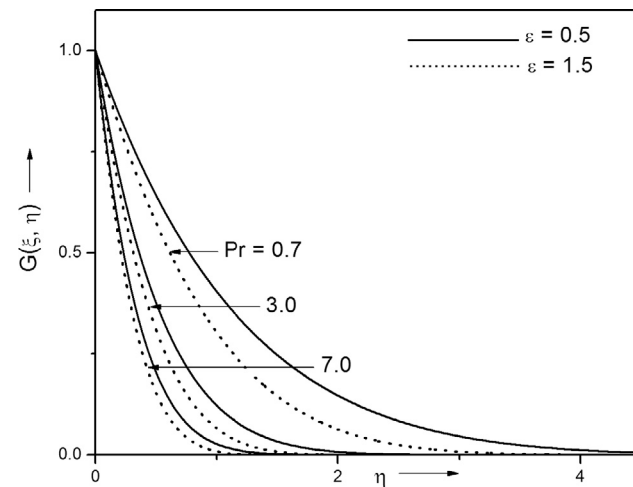


Figure 5 Effects of Pr on temperature $G(\xi, \eta)$ profile for $Ri = 1$, $N = 0.5$, $Sc = 2.57$, $\Delta = 1$, $Re_L = 1$ and $\xi = 0.5$.

coordinate ξ . This indicates that the increase in streamwise coordinate ξ acts as a supporting pressure gradient in the momentum boundary layer and hence fluid moves faster. In particular, for instance, $Ri = 1.0$, $N = 0.5$, $Sc = 2.57$, $\Delta = 1$, $Re_L = 1$, $\varepsilon = 1.5$ and $Pr = 0.7$ at $\eta = 1.0$, the velocity profile increases approximately by 18% as streamwise coordinate ξ increases from $\xi = 0.0$ to $\xi = 1.0$ while temperature profile ($G(\xi, \eta)$) decreases approximately about 62%. The velocity and temperature profiles presented in Fig. 6 also display that both the velocity and thermal gradients at wall increase with the increase in streamwise coordinate ξ . This clearly indicates that the streamwise co-ordinate ξ significantly influences flow, thermal and in turn species concentration fields and displays the existence of non-similarity solutions.

The variations of streamwise coordinate ξ and the ratio of velocity parameter (ε) on the species concentration profile $H(\xi, \eta)$ are depicted in Fig. 7 for $\Delta = 1$, $Ri = 1$, $Re_L = 1$, $Sc = 0.66$, $Pr = 0.7$ and $N = 0.5$. It is observed that species concentration profile $H(\xi, \eta)$ decreases with an increase in

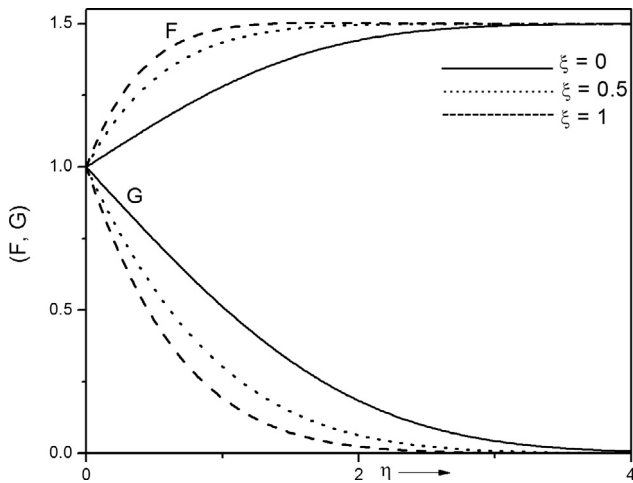


Figure 6 Effects of ξ on velocity $F(\xi, \eta)$ and temperature $G(\xi, \eta)$ profiles for $Ri = 1$, $N = 0.5$, $Pr = 0.7$, $Sc = 2.57$, $\Delta = 1$, $Re_L = 1$ and $\varepsilon = 1.5$.

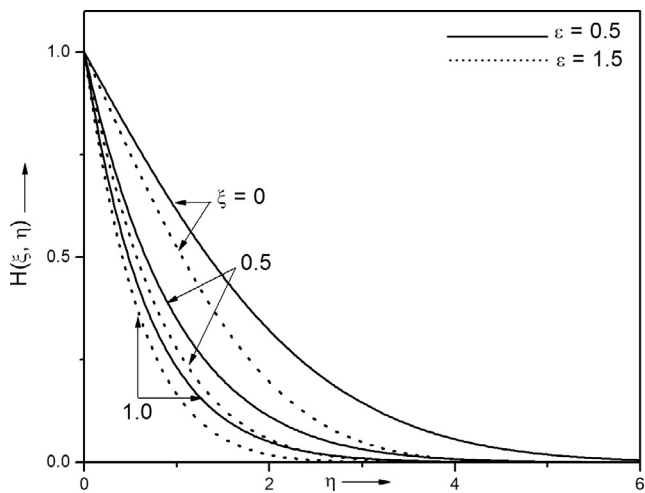


Figure 7 Effects of ξ and ε on concentration $H(\xi, \eta)$ profile for $Ri = 1$, $N = 0.5$, $Pr = 0.7$, $Sc = 0.66$, $\Delta = 1$ and $Re_L = 1$.

streamwise coordinate ξ from $\xi = 0.0$ to $\xi = 1.0$, irrespective values of the ratio of velocity parameter (ε). The reason is that an increase in the streamwise coordinate ξ acts as an adverse pressure gradient in the species concentration profile which reduces the mass diffusion. Thus, in turn, fluid flows become slower. For example, for $Ri = 1.0$, $N = 0.5$, $Sc = 0.66$, $\Delta = 1$, $Re_L = 1$ and $Pr = 0.7$ at $\eta = 1.5$, the species concentration profile decreases approximately about 56% and 61% as streamwise coordinate ξ increases from $\xi = 0.0$ to $\xi = 1.0$ at $\varepsilon = 0.5$ and $\varepsilon = 1.5$, respectively.

Fig. 8 presents the distribution of the species concentration profiles $H(\xi, \eta)$ with the chemical reaction parameter (Δ) and Schmidt number (Sc) for $\varepsilon = 1$, $Pr = 0.7$, $Ri = 1$, $Re_L = 1$, $N = 0.5$ and $\xi = 0.5$. This figure illustrates that species concentration profiles $H(\xi, \eta)$ increase when the species consumption or destructive chemical reaction ($\Delta < 0$) is increased. An increase in $H(\xi, \eta)$ increases the mass diffusion and thus, in turn, the fluid velocity $F(\xi, \eta)$ also increases. Whereas for $\Delta > 0$ (species generation or constructive chemical reaction), the profiles of $H(\xi, \eta)$ tend to decrease and thus, in turn, the fluid velocity is reduced. It should be worthy to mention here that the values of Schmidt number $Sc = 0.22$, 0.66 , 0.94 and 2.57 are chosen to be more realistic, namely, representing diffusing chemical species of most common interest such as water, Propyl Benzene hydrogen and water vapor and Propyl benzene at 25 °C at one atmospheric pressure. It is observed that the magnitude of the species concentration profile $H(\xi, \eta)$ decreases significantly for the increase in Schmidt number (Sc) irrespective values of species consumption or generation. The increase in the value of the Schmidt number Sc leads to a thinning of the concentration boundary layer and the concentration of the fluid decreases within the boundary layer. One can observe that when the species are generated ($\Delta > 0$), the concentration profile $H(\xi, \eta)$ decreases with Δ . However, the opposite trend is observed for the species consumption case ($\Delta < 0$).

The effects of chemical reaction parameter (Δ) and the velocity parameter (ε) on mass transfer parameter ($(Re_L \xi e^\xi)^{-1/2} Sh$) for $Ri = 1.0$, $Pr = 0.7$, $Re_L = 1$, $N = 0.5$ and $Sc = 2.57$ are displayed in Fig. 9. It is observed that the

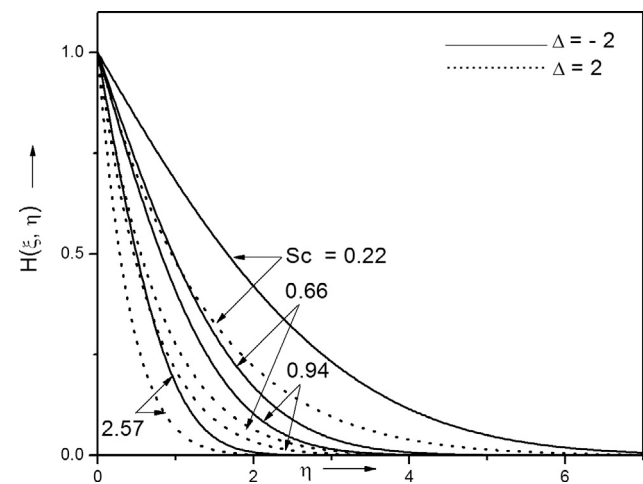


Figure 8 Effects of Δ and Sc on concentration $H(\xi, \eta)$ profile for $Ri = 1$, $N = 0.5$, $Pr = 0.7$, $\varepsilon = 1$, $\xi = 0.5$ and $Re_L = 1$.

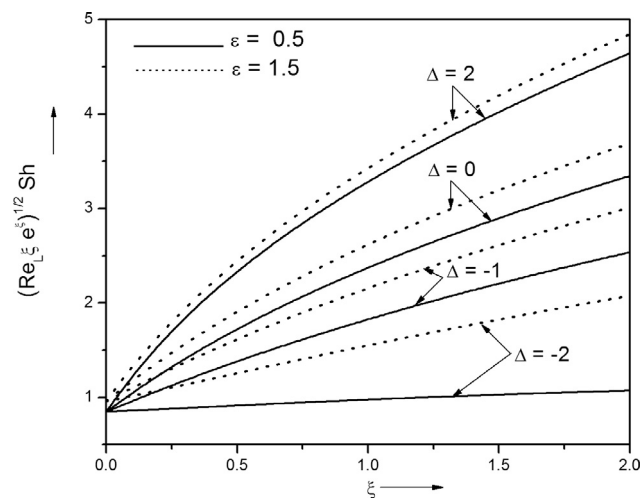


Figure 9 Effects of Δ and ε on mass transfer parameter $(Re_L \xi e^\xi)^{-1/2} Sh$ for $Ri = 1$, $N = 0.5$, $Pr = 0.7$, $Sc = 2.57$ and $Re_L = 1$.

magnitude of the Sherwood number $((Re_L \xi e^\xi)^{-1/2} Sh)$ increases as the chemical reaction parameter (Δ) increases from $\Delta = -2$ to $\Delta = 2$. Also, the results presented in Fig. 9 indicate that $((Re_L \xi e^\xi)^{-1/2} Sh)$ increases with the increase in the velocity ratio parameter. To be more specific, for example, when $Ri = 1$, $Re_L = 1$, $Sc = 2.57$, $Pr = 0.7$ at $\xi = 1.0$, $((Re_L \xi e^\xi)^{-1/2} Sh)$ increases approximately about 59% and 6% as ε increases from 1.0 to 1.5 for $\Delta = -2$ and $\Delta = 2$, respectively (see Fig. 9).

5. Conclusions

In this study, the numerical investigation of a double diffusive mixed convection flow over an impermeable vertical exponentially stretching surface in an exponentially moving free stream in the presence of first order chemical reaction is carried out. The following conclusions are drawn in this numerical investigation:

- In the presence of the buoyancy assisting force ($Ri > 0$), the velocity profile exhibits 25% velocity overshoot for the velocity ratio parameter $\varepsilon < 1$. Further, Richardson number (Ri) tends to increase the magnitude of velocity overshoot for the velocity ratio parameter $\varepsilon > 1$.
- Results indicate that the ratio of buoyancy forces (N) and the ratio of velocity parameter (ε) enhance the skin friction coefficient parameter remarkably up to 35–40%.
- The streamwise coordinate ξ acts like a supporting pressure gradient within the momentum boundary layer and velocity increases approximately about 20% but the thermal and species concentrations decrease about 60% and 56%, respectively.
- The concentration profile $H(\xi, \eta)$ increases when the species consumption or destructive chemical reaction ($\Delta < 0$) is increased. For, $\Delta > 0$ (species generation or constructive chemical reaction), the concentration profiles $H(\xi, \eta)$ decrease and thus, in turn, the fluid velocity is reduced.

Acknowledgment

This work is supported by Major Research Project with ID: MRP-MAJOR-MATH-2013-6619, University Grants Commission, New Delhi 110 002.

One of the Authors' Dr. P. M. Patil expresses his sincere gratitude to Shri Vijaykumar Toragal, Special Secretary to His Excellency Governor of Karnataka State, India for his selfless service to the people of Karnataka State.

References

- [1] Incropera FP, Dewitt DP, Bergman TL, Lavine AS. Fundamentals of heat and mass transfer. 6th ed. New York: John Wiley; 2007.
- [2] Bejan A. Convective heat transfer. 3rd ed. New York: John Wiley & Son; 2004.
- [3] Soundalgekar VM, Murty TVR. Heat transfer in flow past a continuous moving plate with variable temperature. *Wärme Stoffübertr* 1980;14:91–3.
- [4] Ali ME. Heat transfer characteristics of a continuous stretching surface. *Wärme Stoffübertr* 1994;29:227–34.
- [5] Moutsoglou A, Chen TS. Buoyancy effects in boundary layers on inclined continuous, moving sheets. *ASME J Heat Transfer* 1980;102:371–3.
- [6] Magyari E, Keller B. Heat and mass transfer in the boundary layers on an exponentially stretching continuous surface. *J Phys D: Appl Phys* 2000;32:577–85.
- [7] Elbashaeshy EMA. Heat transfer over an exponentially stretching continuous surface with suction. *Arch Mech* 2001;53:643–51.
- [8] Partha MK, Murthy PVS, Rajashekhar GP. Effects of viscous dissipation on the mixed convection heat transfer from an exponentially stretching surface. *Heat Mass Transfer* 2005;41: 360–6.
- [9] Al-Odat MQ, Damesh RA, Al-Azab TA. Thermal boundary layer on an exponentially stretching continuous surface in the presence of magnetic field effect. *Int J Appl Mech Eng* 2006;11:289–99.
- [10] Sajid M, Hayat T. Influence of thermal radiation on the boundary layer flow due to an exponentially stretching sheet. *Int Commun Heat Mass Transfer* 2008;35:347–56.
- [11] Bidin B, Nazar R. Numerical solution of the boundary layer flow over an exponentially stretching sheet with thermal radiation. *Eur J Sci Res* 2009;33:710–7.
- [12] Pal Dulal. Mixed convection heat transfer in the boundary layers on an exponentially stretching surface with magnetic field. *Appl Math Comput* 2010;217:2356–69.
- [13] Ishak A. MHD boundary layer flow due to an exponentially stretching sheet with radiation effect. *Sains Malaysiana* 2011;40: 391–5.
- [14] Mukhopadhyay S, Gorla RSR. Effects of partial slip on boundary layer flow past a permeable exponential stretching sheet in presence of thermal radiation. *Heat Mass Transfer* 2012;48: 1773–81.
- [15] Rehman A, Nadeem S, Malik MY. Boundary layer stagnation-point flow of third grade fluid over an exponentially stretching sheet. *Br J Chem Eng* 2012;30:611–8.
- [16] Rehman Abdul, Nadeem S, Malik MY. Stagnation flow of couple stress nanofluid over an exponentially stretching sheet through a porous medium. *J Power Technol* 2013;93:122–32.
- [17] Rehman A, Nadeem S. Heat transfer analysis of the boundary layer flow over a vertical exponentially stretching cylinder. *Global J Sci Front Res Math Decis Sci* 2013;13:1–14.
- [18] Rehman A, Nadeem S, Malik MY, Naseer M. Nanoparticle effect over the boundary layer flow over an exponentially stretching cylinder. *Proc Inst Mech Eng, Part N: J Nanoeng Nanosyst* 2013:1–6.

- [19] Hayat T, Shehzad SA, Alsaedi A. MHD three dimensional flow by an exponentially stretching surface with convective boundary condition. *J Aerosp Eng* 2014;27, 04014011-8.
- [20] Hayat Tasawar, Ashraf Bilal, Shehzad Sabir Ali, Alsaedi A, Bayomi N. Three dimensional mixed convection flow of viscoelastic nanofluid over an exponentially stretching surface. *Int J Numer Methods Heat Fluid Flow* 2015;25:333-57.
- [21] Hayat Tasawar, Ashraf Bilal, Shehzad Sabir Ali, Abouelmagd Elbaz. Three-dimensional flow of Eyring-Powell nanofluid over an exponentially stretching sheet. *Int J Numer Methods Heat Fluid Flow* 2015;25:593-616.
- [22] Hussain T, Shehzad SA, Alsaedi A, Hayat T, Ramzan M. Flow of Casson nanofluid with viscous dissipation and convective conditions: a mathematical model. *J Central South Univ* 2015;22: 1132-40.
- [23] Shehzad SA, Hayat T, Qasim M, Asghar S. Effects of mass transfer on MHD flow of Casson fluid with chemical reaction and suction. *Br J Chem Eng* 2013;30:187-95.
- [24] Patil PM, Kulkarni PS. Effects of chemical reaction on free convective flow of a polar fluid through a porous medium in the presence of internal heat generation. *Int J Therm Sci* 2008;47: 1043-54.
- [25] Patil PM, Pop I. Effects of surface transfer on unsteady mixed convection flow over a vertical cone with chemical reaction. *Heat Mass Transfer* 2011;47:1453-64.
- [26] Patil PM, Chamkha Ali J, Roy S. Effects of chemical reaction on mixed convection flow of a polar fluid through a porous medium in presence of internal heat generation. *Meccanica* 2012;47: 483-99.
- [27] Hayat Tasawar, Muhammad Taseer, Shehzad Sabir Ali, Alsaedi Ahmed. Temperature and concentration stratification in mixed convection flow of an Oldroyd-B fluid with thermal radiation and chemical reaction. *Plos One* 2015;10:1-23.
- [28] Shehzad SA, Hayat T, Asghar S, Alsaedi A. Stagnation point flow of thixotropic fluid with mass transfer and chemical reaction. *J Appl Fluid Mech* 2015;8:465-71.
- [29] Hayat Tasawar, Muhammad Taseer, Shehzad Sabir Ali, Alsaedi A. Soret and Dufour effects in three-dimensional flow over an exponentially stretching surface with porous medium, chemical reaction and heat source/sink. *Int J Numer Methods Heat Fluid Flow* 2015;25:762-81.
- [30] Hsiao Kai-Long. Heat and mass mixed convection for MHD viscoelastic fluid past a stretching sheet with ohmic dissipation. *Commun Nonlinear Sci Numer Simul* 2010;15:1803-12.
- [31] (Hsiao, 2010) Hsiao Kai-Long. Corrigendum to heat and mass mixed convection for MHD viscoelastic fluid past a stretching sheet with Ohmic dissipation. *Commun Nonlinear Sci Numer Simul* 2010;15:1803-12;
(Hsiao, 2015) Hsiao Kai-Long. Corrigendum to heat and mass mixed convection for MHD viscoelastic fluid past a stretching sheet with Ohmic dissipation. *Commun Nonlinear Sci Numer Simul* 2015;28:232.
- [32] Hsiao Kai-Long. Nanofluid flow with multimedia physical features for conjugate mixed convection and radiation. *Comput Fluids* 2014;104:1-8.
- [33] Hsiao Kai-Long. MHD mixed convection for viscoelastic fluid past a porous wedge. *Int J Non-Linear Mech* 2011;46:1-8.
- [34] Schlichting H, Gersten K. *Boundary layer theory*. New York: Springer; 2000.
- [35] Koleva MN, Vulkov LG. Two-grid quasilinearization approach to odes with applications to model problems in physics and mechanics. *Comput Phys Commun* 2010;181:663-70.
- [36] Patil PM, Roy S, Pop I. Unsteady mixed convection flow over a vertical stretching sheet in a parallel free stream with variable temperature. *Int J Heat Mass Transfer* 2010;53:4741-8.
- [37] Patil PM, Roy S, Pop I. Unsteady effects on mixed convection boundary layer flow from a permeable slender cylinder due to non-linearly stretching. *Comput Fluids* 2012;56:17-23.
- [38] Patil PM. Effects of surface mass transfer on a steady mixed convection flow from a vertical stretching sheet with variable wall temperature and concentration. *Int J Numer Methods Heat Fluid Flow* 2012;22:287-305.
- [39] Varga RS. *Matrix iterative analysis*. USA: Prentice-Hall; 2000.



Dr. Prabhugouda Mallanagouda Patil completed his B.Sc. (1982), M.Sc. (1984) and Ph. D. (1996) degrees from the Karnatak University, Dharwad. Dr. Patil began his teaching career at BLDEA's S.B Arts and KCP Science College, Bijapur-586 103 on Stop-gap basis. Thereafter, he moved on to the BHS Arts and TGP Science College, Jamakhandi - 587 302 on regular basis in 1986 and served there till 1993. Later, Dr. Patil was transferred to JSS's Banashankari Arts, Commerce and Shanti Kumar Gubbi Science College, Vidyagiri, Dharwad - 580 004, and served till October 2013. Currently, Dr. Patil is working in the P.G. Department of Mathematics, Karnatak University, Dharwad. Dr. Patil has worked as a Visiting Scientist from March 1998 to June 1998 at UGC-DSA Centre in Fluid Mechanics, Department of Mathematics, Bangalore University, Bangalore. Dr. Patil was awarded prestigious Commonwealth Academic Fellowship (2011-12) tenable at Department of Mechanical Engineering, University of Bath, United Kingdom. Dr. Patil's research work is interdisciplinary in nature and covers various aspects of Convective Heat and Mass transfer and Computational Fluid Dynamics. His work includes nonsimilar solutions of mixed convection flows of Newtonian and non-Newtonian fluids over various geometries such as vertical cone, vertical slender cylinder, stretching surface, exponentially stretching surface, and flat surface. Dr. Patil was awarded the best Research Publication Award with citation from the Vision Group on Science and Technology, Government of Karnataka, India. The research paper entitled "Unsteady mixed convection flow from a moving vertical plate in a parallel free stream: Influence of heat generation or absorption" for the year 2010 -11 in *Mathematical Sciences*. Dr. Patil has published more than 40 research papers in the ISI indexed with high impact factor journals. Also, Dr. Patil has been visiting many premier research institutions in India for collaborative research such as IIT Chennai, IISc Bangalore, TIFR-CAM Bangalore, University of Delhi.